IJC
International Journal of Cancer

P-glycoprotein (MDR1/ABCB1) controls brain accumulation and intestinal disposition of the novel TGF-β signaling pathway inhibitor galunisertib

Wenlong Li[1], Matthijs Tibben[2], Yaogeng Wang[1], Maria C. Lebre[1], Hilde Rosing[2], Jos H. Beijnen[1,2,3] and Alfred H. Schinkel[1]

[1]The Netherlands Cancer Institute, Division of Pharmacology, Amsterdam, The Netherlands
[2]The Netherlands Cancer Institute, Department of Pharmacy & Pharmacology, Amsterdam, The Netherlands
[3]Utrecht University, Faculty of Science, Department of Pharmaceutical Sciences, Division of Pharmacoepidemiology & Clinical Pharmacology, Utrecht, The Netherlands

Galunisertib (LY2157299), a promising small-molecule inhibitor of the transforming growth factor-beta (TGF-β) receptor, is currently in mono- and combination therapy trials for various cancers including glioblastoma, hepatocellular carcinoma and breast cancer. Using genetically modified mouse models, we investigated the roles of the multidrug efflux transporters ABCB1 and ABCG2, the OATP1A/1B uptake transporters and the drug-metabolizing CYP3A complex in galunisertib pharmacokinetics. *In vitro*, galunisertib was vigorously transported by human ABCB1, and moderately by mouse Abcg2. Orally administered galunisertib (20 mg/kg) was very rapidly absorbed. Galunisertib brain-to-plasma ratios were increased by ~24-fold in *Abcb1a/1b*$^{-/-}$ and *Abcb1a/1b;Abcg2*$^{-/-}$ mice compared to wild-type mice, but not in single *Abcg2*$^{-/-}$ mice, whereas galunisertib oral availability was not markedly affected. However, recovery of galunisertib in the small intestinal lumen was strongly reduced in *Abcb1a/1b*$^{-/-}$ and *Abcb1a/1b;Abcg2*$^{-/-}$ mice. Oral coadministration of the ABCB1/ABCG2 inhibitor elacridar boosted galunisertib brain accumulation in wild-type mice to equal the levels seen in *Abcb1a/1b;Abcg2*$^{-/-}$ mice. Oatp1a/1b deficiency did not alter oral galunisertib pharmacokinetics or liver distribution. *Cyp3a*$^{-/-}$ mice showed a 1.9-fold higher plasma $AUC_{0-1\ hr}$ than wild-type mice, but this difference disappeared over 8 hr. Also, transgenic human CYP3A4 overexpression did not significantly alter oral galunisertib pharmacokinetics. Abcb1 thus markedly restricts galunisertib brain penetration and affects its intestinal disposition, possibly through biliary excretion. Elacridar coadministration could fully inhibit both processes, without causing acute toxicity. Moreover, mouse Cyp3a, but not human CYP3A4, may eliminate galunisertib at high plasma concentrations. These insights may help to guide the further clinical development and application of galunisertib.

Introduction

In the early 1980s, transforming growth factor-beta (TGF-β) ligands including TGF-β1, TGF-β2 and TGF-β3 were identified, all of which regulate diverse biological functions.[1–3] These ligands can independently engage the specific transforming growth factor receptor type I (TGF-βRI/ALK5), which then undergoes dimerization with TGF-βII.[4] This heterodimer complex phosphorylates the intracellular proteins SMAD2 and SMAD3, activating a signaling cascade leading to the nuclear translocation of transcription factor proteins that subsequently induce a range of genes. With the induction of such proteins, the TGFβ signaling pathway plays an important role in tumorigenesis, and contributes

Additional Supporting Information may be found in the online version of this article.
Key words: galunisertib, P-glycoprotein, brain accumulation, intestinal disposition, cytochrome P450-3A, oral availability, Oatp1a/1b
Abbreviations: ABC: ATP-binding cassette; AUC: area under plasma concentration-time curve; BCRP: breast cancer resistance protein; C_{brain}: brain concentration; C_{max}: maximum drug concentration in plasma; CNS: central nervous system; CYP: Cytochrome P450; *Cyp3a*$^{-/-}$: Cyp3a knockout mice; Cyp3aXAV: Cyp3a knockout mice with specific expression of human CYP3A4 in liver and intestine; h (as prefix): human; m (as prefix): mouse; MDCK: Madin–Darby canine kidney; NSCLC: nonsmall cell lung cancer; P_{brain}: relative brain accumulation; P-gp: P-glycoprotein; SI: small intestinal tissue; SIWC: small intestine with content; TGF-β: transforming growth factor-beta; TKI: tyrosine kinase inhibitor; T_{max}: time to reach maximum drug concentration in plasma
Conflict of interest: The research group of Alfred H. Schinkel receives revenue from commercial distribution of some of the mouse strains used in this study.
Grant sponsor: China Scholarship Council (CSC); **Grant number:** 201606220081
DOI: 10.1002/ijc.32568
History: Received 30 Mar 2019; Accepted 9 Jul 2019; Online 15 Jul 2019
Correspondence to: Alfred H. Schinkel, Division of Pharmacology, The Netherlands Cancer Institute, Plesmanlaan 121, 1066 CX Amsterdam, The Netherlands, Tel.: +31-20-512-2046, Fax: +31-20-5121792, E-mail: a.schinkel@nki.nl

What's new?

Galunisertib, a promising small-molecule inhibitor of the TGF-β signaling pathway, is currently in clinical trials for various cancers. Transmembrane transporters and drug-metabolizing enzymes can be important determinants of the pharmacokinetic, efficacy, and safety profiles of drugs. Here, the authors show that galunisertib is transported by the ATP-binding cassette efflux transporter P-glycoprotein/ABCB1, which profoundly restricts brain accumulation and alters intestinal disposition of galunisertib. Pharmacological inhibition of ABCB1 completely reverses these effects. The drug-metabolizing CYP3A complex has a limited role in restricting galunisertib oral availability. The new insights may help optimize the clinical application of galunisertib, especially for brain malignancies.

to the hall-marks of cancer,[5] including tumor proliferation, differentiation, invasion and metastasis, inflammation, angiogenesis and escape of immune surveillance.[3,6,7] Thus, targeting this TGF-β-mediated signal transduction in tumors may provide a novel approach to controlling tumor growth by blocking a central activation node with its connected downstream signaling pathways.[8,9] There are several pharmacological approaches to block TGF-β signaling, including monoclonal antibodies,[10,11] vaccines,[12] antisense oligonucleotides[13] and small molecular inhibitors.[14,15]

Galunisertib (LY2157299 monohydrate, Supporting Information Fig. S1) is a novel oral small-molecule inhibitor of the TGF-β receptor I kinase that specifically downregulates the phosphorylation of SMAD2, abrogating activation of the canonical pathway.[16] Galunisertib showed promising antitumor activity in tumor-bearing animal models for breast, colon and lung cancer and hepatocellular carcinoma.[17] Intriguingly, combination of galunisertib with PD-L1 blockade resulted in improved tumor growth inhibition and complete regression in colon carcinoma models, demonstrating potential synergy when cotargeting TGF-β and PD-1/PD-L1 pathways.[18] Based on a pharmacokinetic/pharmacodynamic model in animals, an intermittent dosing regimen (14 days on/14 days off, on a 28-day cycle) was recommended to obtain an appropriate safety profile in all ongoing trials.[19,20] Galunisertib is being investigated either as monotherapy or in combination with other antitumor regimens (including nivolumab, an anti-PD-1 monoclonal antibody) in patients with cancers with high unmet medical needs such as glioblastoma, pancreatic cancer, hepatocellular carcinoma and nonsmall cell lung cancer (NSCLC). Interestingly, galunisertib recently also emerged from a screen of 5,000 compounds as a drug candidate for treating a broad range of GLIS3-associated diabetic patients.[21]

Transmembrane transporters can be important determinants of the pharmacokinetic, safety and efficacy profiles of drugs.[22] Two major superfamilies, the ATP-binding cassette (ABC) and solute carrier (SLC) transporters have been annotated and studied for decades. The ABC drug efflux transporters P-glycoprotein (P-gp; ABCB1) and breast cancer resistance protein (BCRP; ABCG2) are expressed at the apical membrane of enterocytes, hepatocytes and renal tubular epithelial cells, where they potentially limit intestinal absorption of their substrates or mediate their direct intestinal, hepatobiliary or renal excretion.[23,24] Moreover, ABCB1- and ABCG2-mediated efflux capacity in brain endothelial capillary cells of the blood–brain barrier (BBB) is crucial for the protection of the central nervous system (CNS) from harmful compounds. Conversely, limited exposure of the brain to anticancer drugs because of these transporters may reduce their therapeutic efficacy, especially against brain metastases.[25,26] In addition, ABC transporters are also expressed in many tumor types, potentially mediating multidrug resistance against anticancer drugs.

Organic anion-transporting polypeptides (OATPs; SLCOs) represent a superfamily of uptake transporters which primarily mediate the cellular uptake of various endogenous and exogenous compounds. Members of the OATP1A/1B subfamilies are of interest for their impact on the pharmacokinetics and hence therapeutic efficacy of many drugs due to their wide substrate specificity, and variation in activity due to genetic polymorphisms and drug–drug interactions.[27,28] However, the interaction of galunisertib with the ABCB1, ABCG2 and OATP1A/1B transporters is still largely unknown.

Drug-metabolizing enzymes often work together with the drug transporters in modulating drug absorption, distribution and elimination. Cytochrome P450 3A (CYP3A) is a member of the CYP superfamily and CYP3A enzymes are involved in the metabolism of about 50% of the currently used drugs.[29] CYP3A enzymes display high interindividual and intraindividual variation in activity due to drug–drug interactions and genetic polymorphisms. The plasma exposure and bioavailability of many drugs can therefore be strongly affected by CYP3A activity, which can dramatically influence the therapeutic efficacy in patients. The extent of interaction of CYP3A with galunisertib is currently unclear based on publicly available sources.

We here investigated the *in vivo* roles of the ABCB1, ABCG2 and OATP1A/1B drug transporters in modulating oral availability and/or brain accumulation of galunisertib, using genetically modified mouse models. We also studied to what extent mouse and human CYP3A can impact on the oral availability of galunisertib *in vivo*.

Materials and Methods

Chemicals

Galunisertib was purchased from TargetMol (Boston, MA). Zosuquidar trihydrochloride and elacridar HCl were obtained from Sequoia Research Products (Pangbourne, United Kingdom). Ko143 was from Tocris Bioscience (Bristol, United Kingdom). Bovine Serum Albumin (BSA) Fraction V was obtained from Roche Diagnostics (Mannheim, Germany). Glucose water (5%,

w/v) was from B. Braun Medical Supplies, Inc. (Melsungen, Germany). Isoflurane was purchased from Pharmachemie (Haarlem, The Netherlands), heparin (5,000 IU ml^{-1}) was from Leo Pharma (Breda, The Netherlands). All other chemicals and reagents were obtained from Sigma-Aldrich (Steinheim, Germany).

Cell lines and transport assays

Madin–Darby Canine Kidney (MDCK-II) cells (ECACC 00062107) stably transduced with human (h) ABCB1, hABCG2 or mouse (m) Abcg2 cDNA were previously generated in our institute. These polarized epithelial cells show highly characteristic growth and transport properties, including inhibitor sensitivity, confirming their proper identity. Cells were routinely tested negative for mycoplasma. The passage number when used in transport experiments was 11–16. Transepithelial transport experiments using these cell lines were performed as described in the Supporting Information Material and Methods. Active transport was expressed using the transport ratio *r*, that is, the amount of apically directed drug transport divided by basolaterally directed drug translocation after 4 hr.

Animals

Mice were housed and handled according to institutional guidelines complying with Dutch and EU legislation. Wild-type, *Oatp1a/1b*$^{-/-}$, *Abcb1a/1b*$^{-/-}$, *Abcg2*$^{-/-}$, *Abcb1a/1b; Abcg2*$^{-/-}$, *Cyp3a*$^{-/-}$ and Cyp3aXAV mice, all of a >99% FVB genetic background, were used between 9 and 15 weeks of age. Animals were kept in a temperature-controlled environment with a 12-hr light and 12-hr dark cycle and received a standard diet (Transbreed, SDS Diets, Technilab—BMI, Someren, The Netherlands) and acidified water *ad libitum*.

Drug solutions

For oral administration, galunisertib was dissolved in dimethyl sulfoxide (DMSO) at a concentration of 50 mg/ml and further diluted with pH = 2 (10 mM) hydrochloric acid solution to yield a final galunisertib concentration of 2 mg/ml. Final concentration for DMSO was 4%. Elacridar hydrochloride was dissolved in DMSO (53 mg/ml) in order to obtain 50 mg elacridar base per ml DMSO. The stock solution was further diluted with a mixture of polysorbate 80, ethanol and water (20:13:67, [v/v/v]) to yield a final elacridar concentration of 5 mg/ml. All dosing solutions were prepared freshly on the day of experiment.

Plasma pharmacokinetics and organ distribution of galunisertib in mice

To minimize variation in absorption upon oral administration, mice were fasted for around 2–3 hr before galunisertib (20 mg/kg body weight) was administered by gavage into the stomach at 10 μl/g body weight, using a blunt-ended needle. For the 8 or 1 hr experiments, tail vein blood sampling was performed at 0.25, 0.5, 1, 2 and 4 hr or 5, 10, 20, 30 and 45 min time points after oral administration, respectively, using microvettes containing heparin. Eight or one hour after oral administration, mice were anesthetized with isoflurane and blood was collected by cardiac puncture. Blood samples were collected in Eppendorf tubes containing heparin as an anticoagulant. The mice were then sacrificed by cervical dislocation and brain, liver, spleen, kidneys, lung, small intestine and testis were rapidly removed. The contents of the small intestine were removed, and the tissue quickly rinsed with ice-cold saline before homogenization of the tissue. Organs were homogenized with 4% (w/v) bovine serum albumin. Plasma was isolated from the blood by centrifugation at 9,000*g* for 6 min at 4°C, and the plasma fraction was collected. All samples were stored at −30°C until analysis. Pharmacokinetic parameters for relative organ distributions, pharmacokinetic calculations and statistical analysis were described in the Supporting Information Material and Methods.

Brain accumulation of galunisertib in combination with oral elacridar

Wild-type and *Abcb1a/1b;Abcg2*$^{-/-}$ mice received either elacridar (50 mg/kg body weight) or vehicle orally using 10 μl/g body weight. Then the mice were fasted for around 3.5 hr before 20 mg/kg galunisertib was given by oral administration as described above. Tail vein blood sampling was performed at 2.5, 5, 10 and 20 min after galunisertib administration. Blood, brain, liver and small intestine with content (SIWC) were isolated at the 30 min time point, and processed as described above.

Liquid chromatography coupled with tandem mass spectrometry analysis

Galunisertib concentrations in DMEM cell culture medium, plasma samples and organ homogenates were determined using a sensitive and specific liquid chromatography–tandem mass spectrometry assay.[30]

Data availability

The raw data are available from the corresponding author upon reasonable request.

Results

In vitro transport of galunisertib

Transepithelial transport of galunisertib (5 μM) was tested using polarized monolayers of MDCK-II parental cells and subclones overexpressing hABCB1, hABCG2 or mAbcg2. In the parental MDCK-II cell line, there was high apically directed transport of galunisertib (efflux ratio r = 8.5, Fig. 1*a*), which was strongly reduced by addition of the ABCB1 inhibitor zosuquidar (r = 1.4, Fig. 1*b*). This suggested substantial transport of galunisertib by the low-level endogenous canine ABCB1. Galunisertib was very extensively transported in hABCB1-overexpressing cells (r = 60.0, Fig. 1*c*), and this transport was markedly inhibited by zosuquidar (r = 1.8, Fig. 1*d*).

To evaluate the interaction between ABCG2 and galunisertib, zosuquidar was added to inhibit the endogenous canine ABCB1

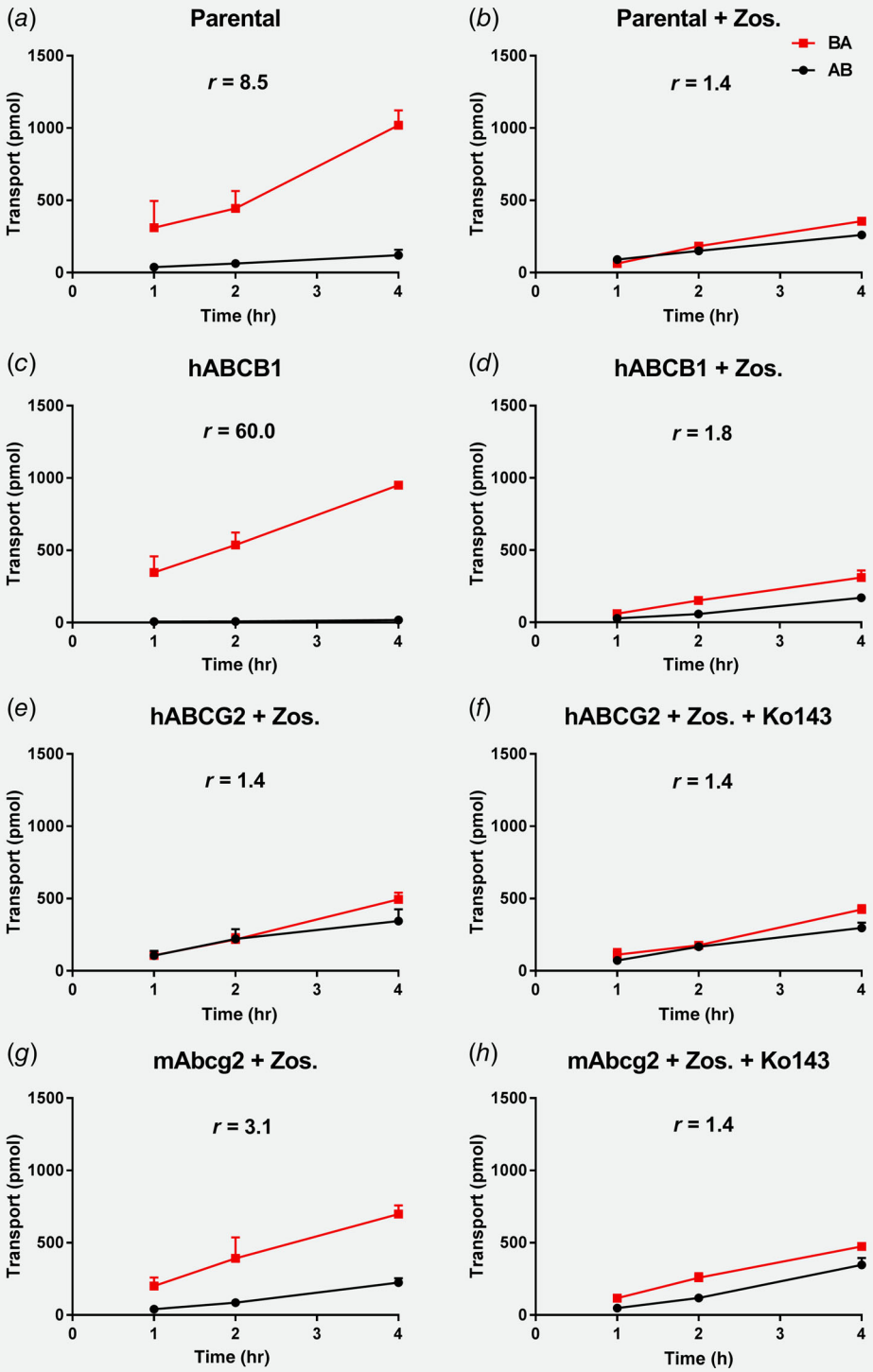

Figure 1. Transepithelial transport of galunisertib (5 μM) assessed in MDCK-II cells either nontransduced (*a*, *b*), transduced with hABCB1 (*c*, *d*), hABCG2 (*e*, *f*) or mAbcg2 (*g*, *h*) cDNA. At $t = 0$ hr, galunisertib was applied in the donor compartment and the concentrations in the acceptor compartment at $t = 1$, 2 and 4 hr were measured and plotted as galunisertib transport (pmol) in the graph ($n = 3$). (*b*, *d*–*h*) Zos. (zosuquidar, 5 μM) was applied to inhibit human and/or endogenous canine ABCB1. (*f*, *h*) The ABCG2 inhibitor Ko143 (5 μM) was applied to inhibit ABCG2/Abcg2-mediated transport. *r*, relative transport ratio. BA (■), translocation from the basolateral to the apical compartment; AB (●), translocation from the apical to the basolateral compartment. Points, mean; bars, SD. [Color figure can be viewed at wileyonlinelibrary.com]

in experiments with MDCK-II cells overexpressing hABCG2 and mAbcg2. Galunisertib was actively transported by cells overexpressing mAbcg2, with a transport ratio of 3.1 (Fig. 1*g*), *vs.* 1.4 in the parental cells. The addition of Ko143, a specific ABCG2 inhibitor, resulted in marked inhibition of this transport (Fig. 1*h*). However, there was no detectable ABCG2-dependent polarized transport of galunisertib in cells overexpressing hABCG2 either with zosuquidar alone or in combination with Ko143 (Figs. 1*e* and 1*f*). Galunisertib thus appears to be very efficiently transported by hABCB1, canine ABCB1 and mAbcg2, but not by hABCG2. Of note, even with zosuquidar and/or Ko143, some apically directed transport was still detectable (Figs. 1*b*, 1*d*, 1*f* and 1*h*, $r \geq 1.4$). This suggests that some other apically directed galunisertib transport system may exist in MDCK-II cells.

Impact of ABCB1 and ABCG2 on galunisertib plasma pharmacokinetics and tissue distribution

To assess a possible impact of mAbcb1a/1b and mAbcg2 on oral availability and tissue distribution of galunisertib, we performed an 8 hr pilot experiment in male wild-type and combination *Abcb1a/1b;Abcg2*$^{-/-}$ mice, using oral administration of 20 mg/kg galunisertib. As shown in Supporting Information Figure S2 and Table S1, oral absorption of galunisertib was very rapid, with the highest concentrations observed already at the earliest time point, 15 min after dosing. Moreover, the half-life of galunisertib in both strains was around 1.2 hr, indicating that galunisertib is rapidly cleared in mice. The plasma area under plasma concentration–time curve ($AUC_{0-8\ hr}$) revealed no significant differences in galunisertib oral availability between wild-type and *Abcb1a/1b;Abcg2*$^{-/-}$ mice.

Brain, liver, spleen, kidney, small intestinal tissue (SI) and testis concentrations of galunisertib were also determined 8 hr after oral administration. We observed substantial increases in brain concentration (19.9-fold) and brain-to-plasma ratio (23.6-fold) in *Abcb1a/1b;Abcg2*$^{-/-}$ mice in comparison with wild-type mice (Supporting Information Figs. S3A–S3C and Table S1). The testis-to-plasma ratio was also 5.2-fold higher in *Abcb1a/1b;Abcg2*$^{-/-}$ mice than in wild-type mice. After log transformation to accommodate the high variation, this modest difference was statistically significant (Supporting Information Table S1 and Fig. S3E). In contrast, exposure of galunisertib in other tested tissues was not much altered between the strains when considering the tissue-to-plasma ratios, except for a borderline significant effect for spleen (Supporting Information Fig. S4).

Whereas galunisertib showed very poor brain penetration in wild-type mice, with extremely low brain-to-plasma ratios (0.033) at 8 hr, in *Abcb1a/1b;Abcg2*$^{-/-}$ mice this was increased to 0.78. Some tyrosine kinase inhibitors (TKIs), such as brigatinib,[26] can cause acute CNS toxicity as a consequence of highly increased brain penetration when ABC transporters are absent or inhibited, resulting in marked behavioral abnormalities and even death. For galunisertib at 20 mg/kg, we did not notice any obvious acute (behavioral) abnormalities in the *Abcb1a/1b;Abcg2*$^{-/-}$ mice.

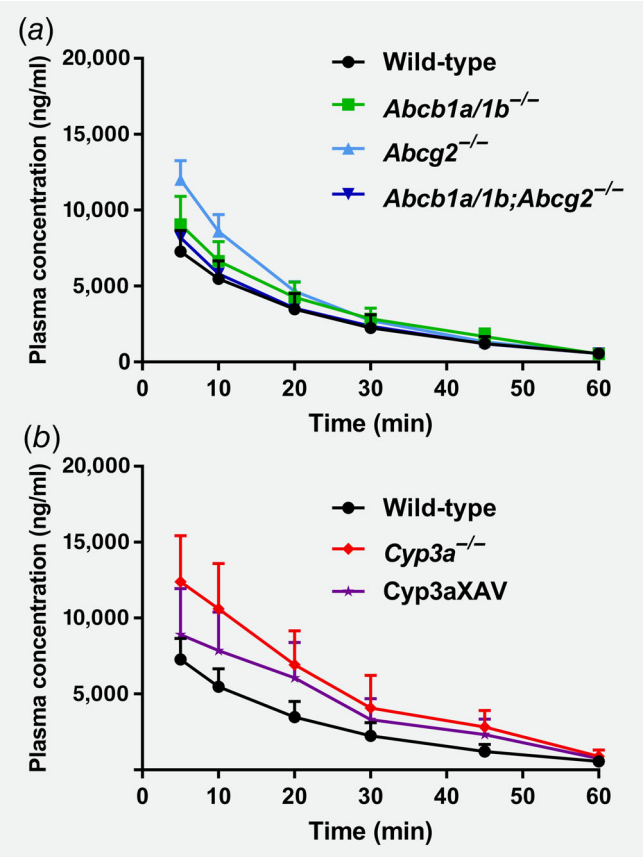

Figure 2. Plasma concentration–time curves of galunisertib in female wild-type, *Abcb1a/1b*$^{-/-}$, *Abcg2*$^{-/-}$, *Abcb1a/1b;Abcg2*$^{-/-}$, *Cyp3a*$^{-/-}$ and Cyp3aXAV mice over 1 hr after oral administration of 20 mg/kg galunisertib. Data are presented as mean ± SD (n = 6–8). Panel *a*: wild-type, *Abcb1a/1b*$^{-/-}$, *Abcg2*$^{-/-}$ and *Abcb1a/1b;Abcg2*$^{-/-}$ mice. Panel *b*: wild-type, *Cyp3a*$^{-/-}$ and Cyp3aXAV mice. [Color figure can be viewed at wileyonlinelibrary.com]

To further investigate the separate and combined roles of mAbcb1a/1b and mAbcg2 in oral availability and tissue disposition of galunisertib, a more extensive experiment was performed terminating at 1 hr, when the plasma levels were still comparatively high. Galunisertib (20 mg/kg) was administered orally to female wild-type, *Abcb1a/1b*$^{-/-}$, *Abcg2*$^{-/-}$ and *Abcb1a/1b;Abcg2*$^{-/-}$ mice. The first blood sample was collected at 5 min but, as shown in Figure 2*a* and Table 1, galunisertib was absorbed extremely quickly, with the time to reach maximum drug concentration in plasma (T_{max}) likely falling even before 5 min. Absence of mAbcg2 resulted in a borderline significant increase in plasma $AUC_{0-1\ hr}$ (1.4-fold) compared to wild-type mice, but, at the same time, there were no significant changes in either *Abcb1a/1b*$^{-/-}$ or *Abcb1a/1b;Abcg2*$^{-/-}$ mice. The *Abcg2*$^{-/-}$ results therefore may represent an outlier at this early stage of oral administration, with often high interindividual variation.

The brain concentration of galunisertib at 1 hr was profoundly increased in *Abcb1a/1b*$^{-/-}$ and *Abcb1a/1b;Abcg2*$^{-/-}$ mice compared to wild-type mice (Fig. 3*a*; Table 1). Similar to the 8 hr data in male mice, the brain-to-plasma ratios were extremely low

Table 1. Plasma and brain pharmacokinetic parameters of galunisertib 1 hr after oral administration of 20 mg/kg galunisertib to female wild-type, *Abcb1a/1b*$^{-/-}$, *Abcg2*$^{-/-}$, *Abcb1a/1b;Abcg2*$^{-/-}$, *Cyp3a*$^{-/-}$ and Cyp3aXAV mice

	Genotype					
Parameter	**Wild-type**	***Abcb1a/1b*$^{-/-}$**	***Abcg2*$^{-/-}$**	***Abcb1a/1b;Abcg2*$^{-/-}$**	***Cyp3a*$^{-/-}$**	**Cyp3aXAV**
$AUC_{0-1\ hr}$, ng/ml hr	2,706 ± 640	3,371 ± 725	3,815 ± 432*	2,858 ± 344	5,181 ± 1,514**	4,095 ± 1,262
Fold change $AUC_{0-1\ hr}$	1.0	1.25	1.40	1.06	1.91	1.51
C_{max}, ng/ml	7,273 ± 1,392	9,065 ± 1,849	12,000 ± 1,255***	8,197 ± 735	12,857 ± 2,931***	9,357 ± 2,372
T_{max}, min	≤5	≤5	≤5	≤5	≤5–10	≤5–20
C_{brain}, ng/g	22.8 ± 12.1	507 ± 121***	26.1 ± 4.0	522 ± 67***	46.8 ± 21.6	23.6 ± 8.2
Fold increase C_{brain}	1.0	22.2	1.1	22.9	2.1	1.0
Brain-to-plasma ratio	0.041 ± 0.009	1.00 ± 0.20***	0.051 ± 0.017	0.97 ± 0.22***	0.053 ± 0.008	0.035 ± 0.008
Fold increase ratio	1.0	24.4	1.2	23.7	1.3	0.9
P_{brain} ($*10^{-3}$ hr^{-1})	8.3 ± 3.0	150 ± 7***	6.8 ± 0.6	183 ± 7***	8.8 ± 2.3	5.7 ± 0.8
Fold increase P_{brain}	1.0	18.1	0.8	22.0	1.1	0.7
C_{liver}, ng/g	2,060 ± 809	1,939 ± 551	1,992 ± 390	1,731 ± 326	2,781 ± 1,085	2,264 ± 875
Fold change C_{liver}	1.0	0.94	0.97	0.84	1.35	1.10
Liver-to-plasma ratio	3.8 ± 0.4	3.8 ± 1.0	3.9 ± 1.1	3.1 ± 0.4	3.3 ± 0.4	3.2 ± 0.5
Fold change ratio	1.0	1.0	1.02	0.82	0.87	0.84
C_{SIC}, µg/g	50.0 ± 23.7	4.5 ± 2.4***	60.2 ± 16.8	6.7 ± 8.5***	68.6 ± 24.9	42.7 ± 17.2
Fold change C_{SIC}	1.0	0.09	1.2	0.13	1.4	0.9
SIC (% of dose)	1.56 ± 1.23	0.07 ± 0.04***	0.86 ± 0.19	0.12 ± 0.16***	0.88 ± 0.44	0.96 ± 0.65
Fold change	1.0	0.04	0.6	0.08	0.6	0.6

Data are presented as mean ± SD (n = 6–8). *p < 0.05; **p < 0.01; ***p < 0.001 compared to wild-type mice.
Abbreviations: $AUC_{0-1\ hr}$, area under the plasma concentration-time curve; C_{max}, maximum concentration in plasma; T_{max}, time point of maximum plasma concentration (range for individual mice); $C_{brain/liver/SIC}$, brain/liver/SIC concentration; P_{brain}, brain accumulation, calculated by determining the galunisertib brain concentration relative to the $AUC_{0-1\ hr}$. SIC (% of dose), drug as percentage of dose present in small intestinal content (SIC).

(0.041) in wild-type mice and these were markedly increased by 24.4- and 23.7-fold due to deficiency of mAbcb1a/1b alone or mAbcb1a/1b and mAbcg2 together, respectively, but not in single *Abcg2*$^{-/-}$ mice (Fig. 3*b*; Table 1). Like at 8 hr, the brain-to-plasma ratios were close to unity in both Abcb1a/1b-deficient strains (Table 1). Unlike in brain, the galunisertib concentration, tissue-to-plasma ratio and tissue accumulation in liver were not significantly different between the strains (Figs. 3*d*–3*f*), and the same applied for spleen and kidney distribution (Supporting Information Fig. S5).

Interestingly, in spite of the relatively early time point after oral administration (1 hr), the concentration and total amount of galunisertib in the small intestinal content was markedly lower in both *Abcb1a/1b*$^{-/-}$ and *Abcb1a/1b;Abcg2*$^{-/-}$ mice compared to the other strains (Figs. 3*g*–3*i*; Table 1). This finding could suggest a more rapid and extensive absorption of galunisertib across the intestinal wall in the absence of intestinal Abcb1a/1b activity (essentially because of loss of an intestinal excretion process), or reduced hepatobiliary recirculation of absorbed galunisertib through biliary excretion of galunisertib mediated by Abcb1a/1b in the bile canaliculi of the liver, or a combination of both processes. The SI concentration of galunisertib followed the profile between the mouse strains seen for the small intestinal content, but at a roughly 10-fold lower concentration level (Supporting Information Figs. S5G–S5I). This is therefore likely primarily a reflection of the intestinal content values.

Collectively, the data indicate that mAbcb1 can profoundly restrict brain distribution of galunisertib and can probably mediate its hepatobiliary and/or direct intestinal excretion. In contrast, mAbcg2 has little or no effect on these processes.

Roles of Oatp1a/1b uptake transporters in galunisertib plasma exposure and liver distribution

OATP-mediated liver uptake can also affect the (oral) availability and elimination of a number of substrate drugs.[27,28] Very little is known about possible interactions of galunisertib with OATP/SLCO uptake transporters. We therefore performed a pilot experiment administering oral galunisertib (20 mg/kg) to female wild-type and *Oatp1a/1b*$^{-/-}$ mice and analyzed the plasma concentrations up to 1 hr as well as the liver-to-plasma ratios at 1 hr. We observed no significant differences between wild-type and *Oatp1a/1b*$^{-/-}$ mice (Supporting Information Figs. 6A and 6B), suggesting that there is no meaningful impact of mouse Oatp1a/1b transporters on galunisertib liver distribution and oral availability.

Roles of CYP3A in galunisertib plasma pharmacokinetics and tissue disposition

Many drugs are extensively metabolized by CYP3A, which can therefore limit the oral availability of its substrates. To assess the interaction between galunisertib and CYP3A, we performed an 8 hr pilot experiment with oral galunisertib at 20 mg/kg in male

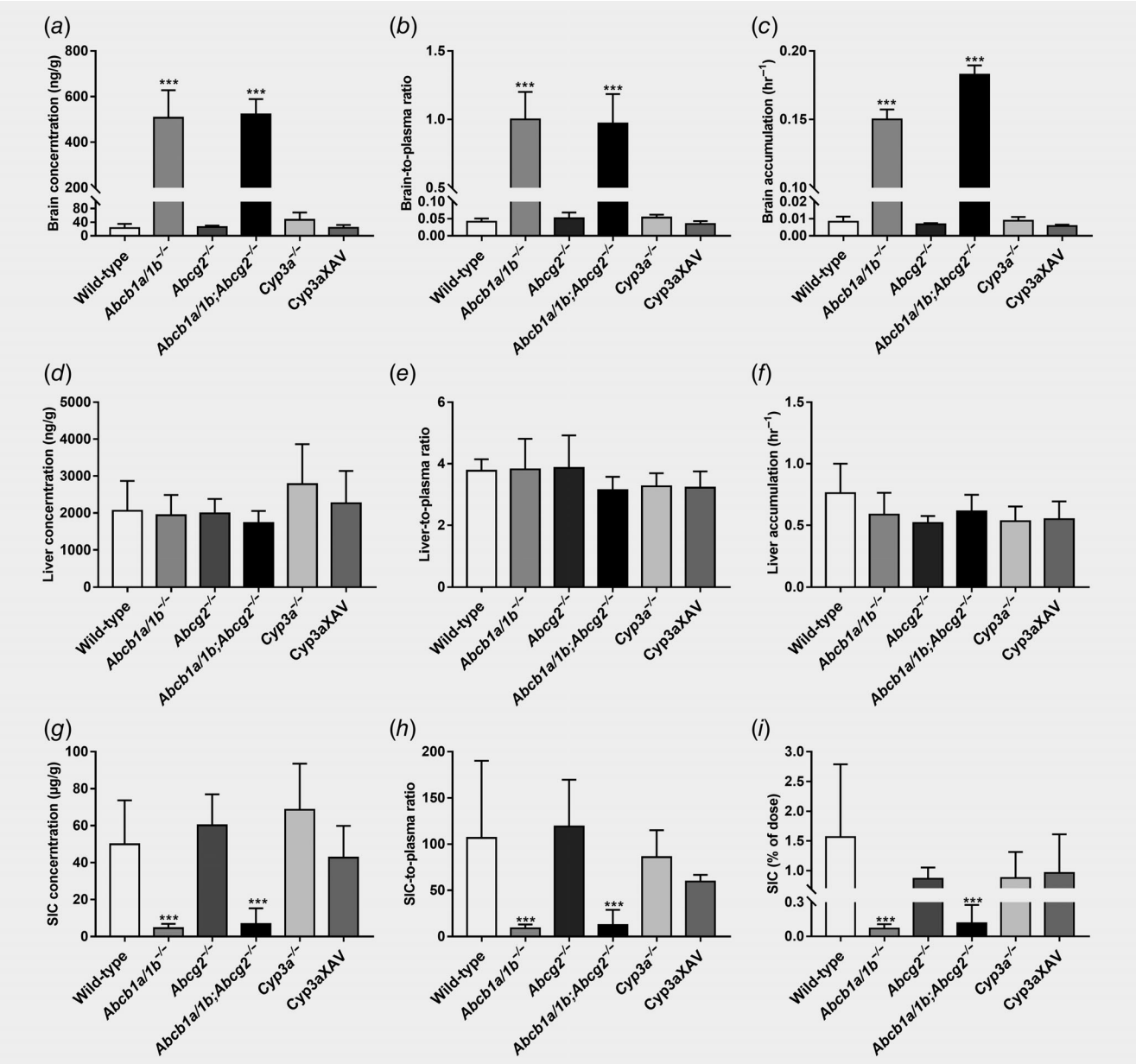

Figure 3. Brain, liver and small intestinal content (SIC) concentration (*a*, *d*, *g*), brain, liver and SIC-to-plasma ratio (*b*, *e*, *h*), brain/liver accumulation (*c*, *f*) and SIC as percentage of dose (*i*) of galunisertib in female wild-type, *Abcb1a/1b*$^{-/-}$, *Abcg2*$^{-/-}$, *Abcb1a/1b;Abcg2*$^{-/-}$, *Cyp3a*$^{-/-}$ and Cyp3aXAV mice 1 hr after oral administration of 20 mg/kg galunisertib. SIC (% of dose), drug percentage of dose in small intestinal content (SIC), which was expressed as total galunisertib in SIC divided by total drug administered to mouse. SIC data were first log-transformed before applying statistical analysis. Data are presented as mean ± SD (n = 6–8). *p < 0.05; **p < 0.01; *** p < 0.001 compared to wild-type mice.

wild-type and *Cyp3a*$^{-/-}$ mice. The highest plasma levels occurred at or before 15 min. Although the maximum drug concentration in plasma (C_{max}) was twofold higher in *Cyp3a*$^{-/-}$ mice than in wild-type mice, no significant differences in plasma $AUC_{0-8\ hr}$ were observed between these two mouse strains (Supporting Information Figs. S2–S4 and Table S1). Moreover, the terminal elimination rate (between 1 and 8 hr) was similar in both strains. Similar to the overall plasma exposure, the relative tissue disposition of galunisertib at 8 hr yielded no noticeable differences between wild-type and *Cyp3a*$^{-/-}$ mice for brain, testis, liver, spleen, kidney and SI (Supporting Information Figs. S3 and S4).

To clarify a possible role of human CYP3A4 in galunisertib pharmacokinetics, in a subsequent 1 hr experiment, we included *Cyp3a*$^{-/-}$ mice with specific transgenic overexpression of human

CYP3A4 in liver and intestine (Cyp3aXAV mice). Blood and tissues were collected 1 hr after oral administration of 20 mg/kg galunisertib to female wild-type, *Cyp3a*$^{-/-}$ and Cyp3aXAV mice. As shown in Figure 2*b* and Table 1, the highest plasma concentrations measured at 5 min were significantly higher (1.7-fold, $p < 0.001$) in *Cyp3a*$^{-/-}$ mice compared to wild-type mice. Moreover, *Cyp3a*$^{-/-}$ mice showed a significantly (1.9-fold) higher ($p < 0.01$) plasma exposure up to 1 hr than wild-type mice (Table 1), qualitatively similar to what we observed during the first hour in the 8-hr experiment (Supporting Information Fig. S2). These results suggest that mCyp3a could restrict systemic exposure of galunisertib at the early stage of distribution/elimination after a dose of 20 mg/kg. The galunisertib oral plasma $AUC_{0-1\ hr}$ in Cyp3aXAV mice was decreased by around 1.3-fold relative to *Cyp3a*$^{-/-}$ mice, but this change was not significant due to the high inter-individual variation. Overall, these data suggest that there may be a limited role of mouse and perhaps human CYP3A in limiting galunisertib plasma levels during the early stages of oral galunisertib disposition.

Effect of the dual ABCB1 and ABCG2 inhibitor elacridar on galunisertib brain accumulation

In view of the poor galunisertib penetration into wild-type brain and the potential benefit of enhancing galunisertib brain accumulation, we investigated to what extent the dual ABCB1 and ABCG2 inhibitor elacridar could increase (boost) brain accumulation of galunisertib. To ensure complete inhibition of the BBB ABC transporters, elacridar (50 mg/kg) or vehicle was administered orally 3.5 hr prior to oral galunisertib administration (20 mg/kg) to wild-type and *Abcb1a/1b;Abcg2*$^{-/-}$ mice. Plasma and brain galunisertib levels were assessed 30 min later. The galunisertib plasma concentration was still quite high at this time point, making the impact of the BBB transporters especially relevant. In the vehicle-treated strains, the galunisertib plasma $AUC_{0-0.5\ hr}$ was not significantly different, and pretreatment with elacridar did not result in significant further alterations in either strain (Supporting Information Fig. S7, Table 2).

In the absence of elacridar, the brain accumulation of galunisertib was 12.8-fold higher in *Abcb1a/1b;Abcg2*$^{-/-}$ mice than in wild-type mice (Fig. 4*c*; Table 2). Elacridar pretreatment markedly increased the brain concentration, brain-to-plasma ratio and brain accumulation of galunisertib in wild-type mice by 10.8-, 12.8- and 12.0-fold, respectively (all $p < 0.001$), resulting in levels similar to those observed in *Abcb1a/1b;Abcg2*$^{-/-}$ mice with or without elacridar pretreatment (Figs. 4*a*–4*c*; Table 2). Since these parameters were not significantly altered by elacridar in *Abcb1a/1b;Abcg2*$^{-/-}$ mice (Figs. 4*a*–4*c*; Table 2), the pharmacokinetic effect of elacridar appears to be specifically mediated by the inhibition of mAbcb1a/1b in the BBB. Unlike for the brain, the liver distribution of galunisertib was not noticeably

Table 2. Plasma, brain, liver and small intestine with content (SIWC) pharmacokinetic parameters of galunisertib 30 min after oral administration of 20 mg/kg galunisertib to female wild-type and *Abcb1a/1b;Abcg2*$^{-/-}$ mice with vehicle or elacridar coadministration

	Genotype and type of pretreatment			
	Vehicle		Elacridar	
Parameter	Wild-type	*Abcb1a/1b;Abcg2*$^{-/-}$	Wild-type	*Abcb1a/1b;Abcg2*$^{-/-}$
$AUC_{0-0.5\ hr}$, ng/ml hr	3,390 ± 943	4,620 ± 880	3,144 ± 631	3,919 ± 833
Fold change $AUC_{0-0.5\ hr}$	1.0	1.36	0.93	1.16
C_{max}, μg/ml	12.1 ± 3.4	14.3 ± 2.4	11.2 ± 2.8	13.8 ± 3.5
T_{max}, min	≤2.5–5	≤2.5–5	≤2.5–5	≤2.5–5
C_{brain}, ng/g	100.0 ± 53.2	1,682 ± 299***	1,082 ± 260***	1,553 ± 346***
Fold increase C_{brain}	1.0	16.8	10.8	15.5
Brain-to-plasma ratio	0.038 ± 0.008	0.39 ± 0.11***	0.49 ± 0.16***	0.51 ± 0.12***
Fold increase ratio	1.0	10.3	12.9	13.4
P_{brain} ($*10^{-3}$ hr^{-1})	28.63 ± 8.67	366.0 ± 27.1***	343.1 ± 38.1***	397.1 ± 45.9***
Fold increase P_{brain}	1.0	12.8	12.0	13.9
Liver-to-plasma ratio	2.74 ± 0.54	2.26 ± 0.60	3.06 ± 0.83	2.79 ± 0.26
Fold change ratio	1.0	0.82	1.12	1.02
C_{SIWC}, μg/ml	53.7 ± 14.8	12.0 ± 2.5***	8.8 ± 2.1***	12.3 ± 2.5***
Fold change C_{SIWC}	1.0	0.22	0.16	0.23
SIWC-to-plasma ratio	21.9 ± 4.7	2.92 ± 1.45***	3.95 ± 1.28***	4.07 ± 0.92***
Fold change ratio	1.0	0.13	0.18	0.19
P_{SIWC} ($*hr^{-1}$)	16.3 ± 3.16	2.70 ± 0.94***	2.92 ± 1.12***	3.26 ± 1.07***
Fold increase P_{SWIC}	1.0	0.17	0.18	0.20

Data are presented as mean ± SD ($n = 7$). Galunisertib was administered alone or coadministered with 50 mg/kg oral elacridar 3.5 hr prior to galunisertib administration. *$p < 0.05$; **$p < 0.01$; ***$p < 0.001$ compared to vehicle-treated wild-type mice.

Abbreviations: $AUC_{0-0.5\ hr}$, area under the plasma concentration–time curve; C_{max}, maximum concentration in plasma; T_{max}, time point of maximum plasma concentration; SIWC, small intestine with content; $C_{brain/SIWC}$, brain/SIWC concentration; $P_{brain/SIWC}$, brain/SIWC accumulation.

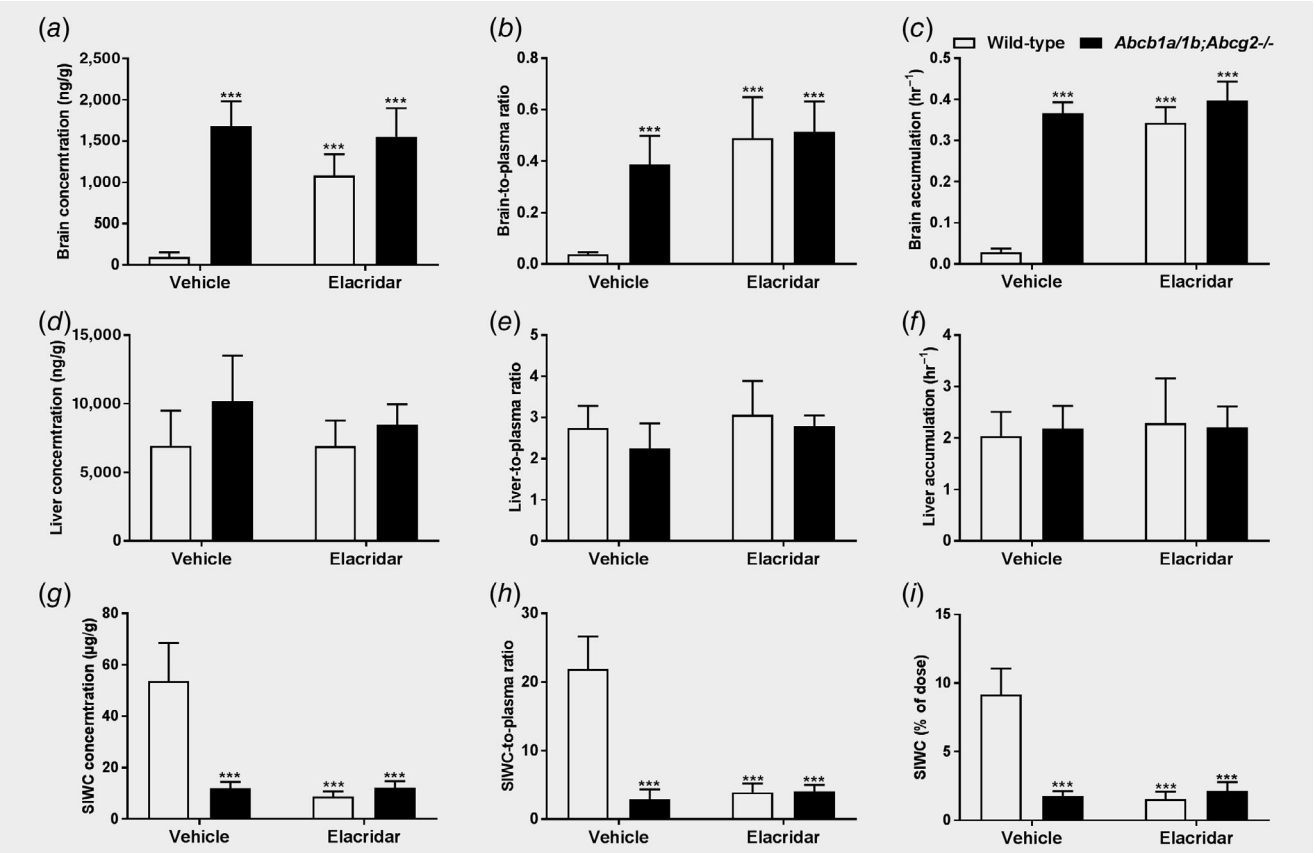

Figure 4. Brain, liver, small intestine with content (SIWC) concentrations (*a*, *d*, *g*), brain, liver and SIWC-to-plasma ratios (*b*, *e*, *h*), brain/liver accumulations (*c*, *f*) and SIWC as percentage of dose (*i*) of galunisertib in female wild-type (white bars) and *Abcb1a/1b;Abcg2*$^{-/-}$ mice (black bars) 30 min after oral administration of 20 mg/kg galunisertib without or with oral elacridar (50 mg/kg) coadministration. Data are presented as mean ± SD ($n = 7$). *$p < 0.05$; **$p < 0.01$; *** $p < 0.001$ compared to vehicle-treated wild-type mice.

affected by elacridar treatment in either mouse strain (Figs. 4*d*–4*f*, Table 2).

Elacridar coadministration resulted in a pronounced, ~sixfold decrease in concentration and total amount of galunisertib present in the small intestine combined with content (SIWC) in wild-type mice, yielding levels similar to those observed in *Abcb1a/1b;Abcg2*$^{-/-}$ mice (Figs. 4*g*–4*i*; Table 2). In wild-type mice, 9.2% of the dose was recovered in SIWC, and in *Abcb1a/1b;Abcg2*$^{-/-}$ mice just 1.8% (Fig. 4*i*; Table 2). No significant differences in galunisertib SIWC distribution were observed between elacridar-treated wild-type mice and vehicle- or elacridar-treated *Abcb1a/1b;Abcg2*$^{-/-}$ mice. This suggests that the mouse Abcb1 in the small intestine and/or the bile canaliculi of the liver was completely inhibited by elacridar, resulting in decreased recovery of galunisertib in the SIWC.

Discussion

In our study, we found that the TGF-β pathway inhibitor galunisertib is an excellent *in vitro* transport substrate of human ABCB1 and canine ABCB1, and a modest substrate of mouse Abcg2, but not of human ABCG2. Upon oral administration to wild-type, *Abcb1a/1b*$^{-/-}$, *Abcg2*$^{-/-}$ and *Abcb1a/1b;Abcg2*$^{-/-}$ mice, galunisertib was very rapidly absorbed in all mouse strains, but no strong effects of Abcb1a/1b and/or Abcg2 deficiencies were observed on the oral availability of galunisertib. However, brain accumulation of galunisertib was dramatically increased in *Abcb1a/1b*$^{-/-}$ (18.1-fold) and *Abcb1a/1b;Abcg2*$^{-/-}$ mice (22-fold), but not in *Abcg2*$^{-/-}$ mice. Similar effects were observed at 0.5, 1 and 8 hr after galunisertib administration. This indicates that ABCB1 P-glycoprotein in the BBB can profoundly restrict the brain penetration of galunisertib. Moreover, we also found a markedly lower concentration and total amount of galunisertib in the small intestine and its contents in the absence of Abcb1a/1b, suggesting that P-glycoprotein can mediate hepatobiliary excretion of galunisertib or direct efflux of galunisertib across the intestinal wall, or a combination of both processes. In contrast, galunisertib distribution to other tissues, with the possible exception of testis, was not noticeably affected by the ABC transporter deficiencies. The impact of mAbcg2 appears to be negligible on both brain distribution and enterohepatic circulation of galunisertib. Coadministration of the ABCB1/ABCG2 inhibitor elacridar fully reversed the impact of Abcb1 on brain accumulation and intestinal disposition of galunisertib. We further found that galunisertib oral availability in mice was somewhat limited by mouse Cyp3a early after oral

administration, but not by human CYP3A4, suggesting that at this early absorption/distribution phase mouse Cyp3a can play a limited role in the metabolic clearance of galunisertib. The mouse Oatp1a/1b transporters did not have a significant impact on the oral availability and liver distribution of galunisertib.

With oral administration of galunisertib at 20 mg/kg to mice, we obtained a plasma exposure in the same range as seen for the steady-state plasma AUC in man.[31] The galunisertib absorption phase in all tested mouse strains was comparable and extremely fast. Our *in vitro* study indicates that mAbcg2 could modestly transport galunisertib with an efflux ratio of 3.1 (Fig. 1*g*). In the absence of mAbcg2, we observed a 1.4-fold higher plasma AUC compared to wild-type mice, but this shift was lost when mAbcb1 was also knocked out. These results may therefore represent an outlier at this early stage of oral administration, with often high interindividual variations. Overall, there does not seem to be a substantial impact of Abcb1a/1b and/or Abcg2 on the oral availability of galunisertib.

Galunisertib shows promising antitumor activity in tumor-bearing mouse models for breast, lung and colon cancer and hepatocellular carcinoma.[17] Given the importance of readily reaching brain metastases in NSCLC and breast cancer, the interaction between ABC transporters in the BBB and galunisertib should be thoroughly studied. Adkin *et al.*[32] showed that treatment with galunisertib reduced the number of tumor cells and extravasation across the BBB, which translated to development of fewer metastases and increased survival in a mouse model with brain metastasis of breast cancer. While we find low brain penetration of galunisertib in wild-type mice, with a brain-to-plasma ratio of 0.041, this penetration could be dramatically enhanced by around 24-fold by the removal of Abcb1 P-glycoprotein in the BBB (Fig. 3*b*; Table 1). Compared to a panel of 12 other TKIs, we investigated previously, galunisertib showed low intrinsic brain penetration in wild-type mice, ranking fourth lowest. However, the 24-fold increase in *Abcb1a/1b;Abcg2*$^{-/-}$ mice ranked fourth highest in this panel, showing a relatively strong impact of Abcb1 on the brain accumulation of galunisertib.

Considering the very limited brain penetration of galunisertib observed in wild-type mice due to Abcb1 function, and its potential relevance for limiting therapeutic efficacy against brain metastases and tumor cells that themselves express ABCB1, we further focused on ways to improve the brain concentration of galunisertib. Elacridar has been extensively used as an ABCB1 and ABCG2 inhibitor to boost the passage of substrate molecules across the BBB into the brain.[25,26] The T_{max} of oral elacridar is around 4 hr in mice.[33] Elacridar was therefore administered prior to a 3.5 hr-fasting period, and then galunisertib was administered, aiming to obtain an optimally efficient inhibition 0.5 hr later. We could indeed completely reverse the impact of Abcb1 on restricting the brain distribution of galunisertib (Fig. 4). We thus demonstrated that virtually complete inhibition of Abcb1 in the BBB could be achieved using a clinically realistic coadministration schedule.

The lack of effect of elacridar on brain accumulation and small intestine concentration of galunisertib in the *Abcb1a/1b;Abcg2*$^{-/-}$ mice further suggests that other uptake or efflux systems for galunisertib were not noticeably affected by elacridar at this dose (Fig. 4; Table 2). Moreover, while some TKI drugs such as brigatinib can cause acute and severe CNS toxicity when Abcb1a/1b and Abcg2 in the BBB are ablated or inhibited,[26] we did not observe any spontaneous CNS toxicity signs for galunisertib in *Abcb1a/1b;Abcg2*$^{-/-}$ or elacridar-treated wild-type mice. After further preclinical and clinical assessment, our findings could therefore potentially provide a rationale for improved treatment for brain metastases and also primary brain tumors by using coadministration of galunisertib with an efficacious ABCB1 inhibitor.

Galunisertib is also being investigated in combination with previously registered anticancer drugs in patients with hepatocellular carcinoma (sorafenib, NCT02240433) and breast cancer (paclitaxel, NCT02672475). According to the FDA documentation, sorafenib is an inhibitor of ABCB1 P-gp.[34] Given the marked drug–drug interaction between galunisertib and elacridar, any attempt to apply efficacious ABCB1/ABCG2 inhibitors in patients in order to improve the CNS and tumor penetration of galunisertib should be carefully monitored, even though no noticeable signs of acute galunisertib CNS toxicity were observed in our study.

Interestingly, the small intestinal contents in Abcb1a/1b-deficient mice showed markedly lower galunisertib concentrations compared to wild-type mice at 60 and 30 min after drug administration (Figs. 3 and 4). Such pronounced effects of P-glycoprotein on enterohepatic cycling of drugs are not often observed shortly after oral administration, because usually the amount of administered drug still residing in the intestinal lumen obscures any contribution of biliary and/or direct intestinal excretion. However, the fact that galunisertib has an extremely rapid absorption profile in mice, with a T_{max} earlier than 5 min, may have reduced the intestinal content of galunisertib fast enough to allow detection of the biliary and/or intestinal excretion component. As discussed below, there are reasonable, albeit speculative explanations for the combination of observations we made.

The rapid oral absorption of galunisertib suggests that there are high-capacity uptake systems for galunisertib in the intestinal epithelium of mice. While the identity of these putative transport systems is unknown, the gut has evolved to absorb a huge variety of nutrients, so there may be several candidates. The resulting high intestinal influx of galunisertib initially likely overwhelms the efflux activity of Abcb1a/1b, explaining why we see little or no impact of Abcb1a/1b deficiency on the oral availability of galunisertib.

To explain the decreased intestinal content amount of galunisertib in Abcb1a/1b-deficient mice after 30–60 min, we speculate that there may be hepatobiliary excretion and/or direct intestinal excretion of galunisertib ongoing in wild-type mice by Abcb1a/1b that is reduced in the knockout mice. Yet, the liver

accumulation of galunisertib was not increased in the Abcb1a/1b knockout mice, which seems to contradict a pronounced decrease in biliary excretion. However, intrahepatic bile (without the gall bladder) can represent a few percent of the total liver volume, and P-glycoprotein substrates may be concentrated 50–100 fold in the bile. An increase in liver parenchyma cell galunisertib concentration in the Abcb1a/1b knockout mice may thus be offset by a decrease in biliary concentration, resulting in no significant change in the overall liver accumulation. Also direct intestinal excretion (or reduced absorption) mediated by Abcb1a/1b might play a role in enhancing intestinal content drug concentrations, once the intraluminal concentrations of galunisertib have dropped and the Abcb1a/1b transport capacity is no longer saturated.

In contrast to the gut epithelium, the BBB is highly selective, and generally allows only the mediated uptake of specific nutrients and signaling molecules essential for brain function. The low brain penetration of galunisertib suggests that any intestinal-type uptake systems for galunisertib are absent from the BBB, or only lowly expressed. The low overall uptake rate of galunisertib across the BBB makes it far easier for Abcb1a/1b in the BBB to effectively counteract this influx. Furthermore, the galunisertib blood concentrations to which the BBB is exposed are likely far lower than the intestinal luminal concentrations of galunisertib shortly after oral administration. It could thus be that intestinal Abcb1a/1b is then completely saturated, whereas BBB Abcb1a/1b is not.

To date, very little information is publicly available on the possible interaction of galunisertib with CYP3A. Using mechanistic static modeling with the CYP3A4 inhibitor itraconazole, Cassidy *et al.*[35] suggested that the clearance of galunisertib was primarily mediated by CYP3A4. However, metabolite formation was very low after 24 hr incubation with pooled human hepatocytes cocultured with murine stromal cells. This is inconsistent with the short half-life and rapid elimination of galunisertib we observed in mice or as reported by a previous study.[17] In our study, we observed a somewhat (1.9-fold) higher plasma $AUC_{0-1\ hr}$ in $Cyp3a^{-/-}$ mice, but this difference disappeared as the plasma concentrations went down, and was not noticeable anymore when considering the plasma $AUC_{0-8\ hr}$. This suggests that other elimination pathways are also importantly involved in galunisertib clearance, and may play a more dominant role at lower plasma concentrations. These alternative elimination systems for galunisertib could perhaps be saturated when the plasma concentrations of galunisertib are high, and then the role of mouse Cyp3a becomes noticeable. Furthermore, no significant decrease in plasma exposure of galunisertib was observed due to the presence of human CYP3A4 in liver and intestine of $Cyp3a^{-/-}$ mice. This suggests that human CYP3A4 plays little, if any, role in the elimination of galunisertib. Based on these findings, coadministration of CYP3A4 inhibitors or inducers may therefore be unlikely to substantially alter the pharmacokinetics of galunisertib in patients, but this will need to be carefully assessed in humans first. In future studies, it will further be of interest to try and identify the molecular nature of the alternative elimination systems for galunisertib in mice and possibly humans.

To the best of our knowledge, this is the first study documenting that galunisertib is significantly transported by both ABCB1 and ABCG2 *in vitro*, and that its brain accumulation, but not oral availability, is primarily and markedly restricted by ABCB1 (P-glycoprotein) in mice. Additionally, the absence of P-glycoprotein diminished hepatobiliary or direct intestinal excretion of galunisertib into the lumen of the small intestine, thus affecting the enterohepatic cycling of galunisertib. However, this had no significant impact on the overall oral availability. Furthermore, mouse Cyp3a and perhaps human CYP3A4 appear to have at best a limited role in restricting plasma levels during the early stages of oral galunisertib pharmacokinetics. Coadministration of elacridar could profoundly improve the brain distribution of oral galunisertib, without altering systemic exposure or causing apparent CNS toxicity. The insights obtained from our study may be useful to further enhance the therapeutic application and efficacy of galunisertib.

References

1. Roberts AB, Anzano MA, Lamb LC, et al. New class of transforming growth factors potentiated by epidermal growth factor: isolation from non-neoplastic tissues. *Proc Natl Acad Sci USA* 1981; 78:5339–43.
2. Piek E, Heldin CH, Ten Dijke P. Specificity, diversity, and regulation in TGF-beta superfamily signaling. *FASEB J* 1999;13:2105–24.
3. Massague J, Blain SW, Lo RS. TGFbeta signaling in growth control, cancer, and heritable disorders. *Cell* 2000;103:295–309.
4. Cheifetz S, Weatherbee JA, Tsang ML, et al. The transforming growth factor-beta system, a complex pattern of cross-reactive ligands and receptors. *Cell* 1987;48:409–15.
5. Hanahan D, Weinberg RA. Hallmarks of cancer: the next generation. *Cell* 2011;144:646–74.
6. Siegel PM, Massague J. Cytostatic and apoptotic actions of TGF-beta in homeostasis and cancer. *Nat Rev Cancer* 2003;3:807–21.
7. Pickup M, Novitskiy S, Moses HL. The roles of TGFbeta in the tumour microenvironment. *Nat Rev Cancer* 2013;13:788–99.
8. Biswas S, Criswell TL, Wang SE, et al. Inhibition of transforming growth factor-beta signaling in human cancer: targeting a tumor suppressor network as a therapeutic strategy. *Clin Cancer Res* 2006;12:4142–6.
9. Akhurst RJ, Hata A. Targeting the TGFbeta signalling pathway in disease. *Nat Rev Drug Discov* 2012;11:790–811.
10. Morris JC, Tan AR, Olencki TE, et al. Phase I study of GC1008 (fresolimumab): a human anti-transforming growth factor-beta (TGFbeta) monoclonal antibody in patients with advanced malignant melanoma or renal cell carcinoma. *PLoS One* 2014;9:e90353.
11. Zhong Z, Carroll KD, Policarpio D, et al. Anti-transforming growth factor beta receptor II antibody has therapeutic efficacy against primary tumor growth and metastasis through multieffects on cancer, stroma, and immune cells. *Clin Cancer Res* 2010;16:1191–205.
12. Giaccone G, Bazhenova LA, Nemunaitis J, et al. A phase III study of belagenpumatucel-L, an allogeneic tumour cell vaccine, as maintenance therapy for non-small cell lung cancer. *Eur J Cancer (Oxford, England : 1990)* 2015;51:2321–9.
13. Jaschinski F, Rothhammer T, Jachimczak P, et al. The antisense oligonucleotide trabedersen (AP 12009) for the targeted inhibition of TGF-beta2. *Curr Pharm Biotechnol* 2011;12: 2203–13.
14. Sawyer JS, Anderson BD, Beight DW, et al. Synthesis and activity of new aryl- and heteroaryl-substituted pyrazole inhibitors of the transforming growth factor-beta type I receptor kinase domain. *J Med Chem* 2003;46:3953–6.
15. Jin CH, Krishnaiah M, Sreenu D, et al. Discovery of N-((4-([1,2,4]triazolo[1,5-a]pyridin-6-yl)-

5-(6-methylpyridin-2-yl)-1H-imidazol-2-yl) methyl)-2-fluoroaniline (EW-7197): a highly potent, selective, and orally bioavailable inhibitor of TGF-beta type I receptor kinase as cancer immunotherapeutic/antifibrotic agent. *J Med Chem* 2014;57:4213–38.
16. Bueno L, de Alwis DP, Pitou C, et al. Semi-mechanistic modelling of the tumour growth inhibitory effects of LY2157299, a new type I receptor TGF-beta kinase antagonist, in mice. *Eur J Cancer (Oxford, England: 1990)* 2008;44: 142–50.
17. Herbertz S, Sawyer JS, Stauber AJ, et al. Clinical development of galunisertib (LY2157299 monohydrate), a small molecule inhibitor of transforming growth factor-beta signaling pathway. *Drug Des Devel Ther* 2015;9:4479–99.
18. Holmgaard RB, Schaer DA, Li Y, et al. Targeting the TGFbeta pathway with galunisertib, a TGFbetaRI small molecule inhibitor, promotes anti-tumor immunity leading to durable, complete responses, as monotherapy and in combination with checkpoint blockade. *J Immunother Cancer* 2018;6:47.
19. Yingling J. Targeting the TGF-β RI kinase with LY2157299: A PK/PD-driven drug discovery and clinical development program. *Proc Amer Assoc Cancer Res* 2005;65:1463.
20. Rodon J, Carducci MA, Sepulveda-Sanchez JM, et al. First-in-human dose study of the novel transforming growth factor-beta receptor I kinase inhibitor LY2157299 monohydrate in patients with advanced cancer and glioma. *Clin Cancer Res* 2015;21:553–60.
21. Amin S, Cook B, Zhou T, et al. Discovery of a drug candidate for GLIS3-associated diabetes. *Nat Commun* 2018;9:2681.
22. Nigam SK. What do drug transporters really do? *Nat Rev Drug Discov* 2015;14:29–44.
23. Borst P, Elferink RO. Mammalian ABC transporters in health and disease. *Annu Rev Biochem* 2002;71:537–92.
24. Schinkel AH, Jonker JW. Mammalian drug efflux transporters of the ATP binding cassette (ABC) family: an overview. *Adv Drug Deliv Rev* 2003;55:3–29.
25. Li W, Sparidans RW, Wang Y, et al. P-glycoprotein (MDR1/ABCB1) restricts brain accumulation and cytochrome P450-3A (CYP3A) limits oral availability of the novel ALK/ROS1 inhibitor lorlatinib. *Int J Cancer* 2018;143:2029–38.
26. Li W, Sparidans RW, Wang Y, et al. P-glycoprotein and breast cancer resistance protein restrict brigatinib brain accumulation and toxicity, and, alongside CYP3A, limit its oral availability. *Pharmacol Res* 2018;137:47–55.
27. van de Steeg E, Wagenaar E, van der Kruijssen CM, et al. Organic anion transporting polypeptide 1a/1b-knockout mice provide insights into hepatic handling of bilirubin, bile acids, and drugs. *J Clin Invest* 2010;120:2942–52.
28. Iusuf D, van Esch A, Hobbs M, et al. Murine Oatp1a/1b uptake transporters control rosuvastatin systemic exposure without affecting its apparent liver exposure. *Mol Pharmacol* 2013; 83:919–29.
29. Thelen K, Dressman JB. Cytochrome P450-mediated metabolism in the human gut wall. *J Pharm Pharmacol* 2009;61:541–58.
30. Tibben MM, Huijberts S, Li W, et al. Liquid chromatography-tandem mass spectrometric assay for the quantification of galunisertib in human plasma and the application in a pre-clinical study. *J Pharm Biomed Anal* 2019;173:169–75.
31. Rodon J, Carducci M, Sepulveda-Sanchez JM, et al. Pharmacokinetic, pharmacodynamic and biomarker evaluation of transforming growth factor-beta receptor I kinase inhibitor, galunisertib, in phase 1 study in patients with advanced cancer. *Invest New Drugs* 2015;33:357–70.
32. Adkins CE, Nounou MI, Mittapalli RK, et al. A novel preclinical method to quantitatively evaluate early-stage metastatic events at the murine blood-brain barrier. *Cancer Prev Res (Phila)* 2015;8:68–76.
33. Kemper EM, Jansen B, Brouwer KR, et al. Bioanalysis and preliminary pharmacokinetics of the acridonecarboxamide derivative GF120918 in plasma of mice and humans by ion-pairing reversed-phase high-performance liquid chromatography with fluorescence detection. *J Chromatogr B Biomed Sci Appl* 2001;759:135–43.
34. FDA. Center for Drug Evaluation and Research of the US Department of Health and Human Service, Food and Drug Administration. Multi-discipline review. Available from: https://www.accessdata.fda.gov/drugsatfda_docs/label/2010/021923s008s009lbl.pdf 2010.
35. Cassidy KC, Gueorguieva I, Miles C, et al. Disposition and metabolism of [(14)C]-galunisertib, a TGF-betaRI kinase/ALK5 inhibitor, following oral administration in healthy subjects and mechanistic prediction of the effect of itraconazole on galunisertib pharmacokinetics. *Xenobiotica* 2018;48:382–99.